Optimization of complex 3-D PM machines in Excel-Visual Basic-MagNet3D environment: case of the Clawpole Transverse Flux Machine

Maxime R. Dubois[*1] Nicolas Dehlinger[*2] Joao P. Trovao[*1]
Professor, Department of Electrical & Computer Engineering, Université de Sherbrooke [*1]
e-TESC Lab, Canada - (819) 821 8000 x 62687, maxime.dubois@usherbrooke.ca
GE Renewables, Denver, CO [*2]

1. Introduction

TRANSVERSE flux machines (TFMs) are known for their high power and torque density capabilities [1]. It is expected that TFMs will find their applications in some low-speed high torque direct drive applications such as wind turbine generators or traction motors for electric vehicles [2]. Since its introduction by Weh in 1986 [1], several structures have been proposed with the transverse flux concept such as single- or double-sided machines, TFMs with surface magnets or with flux concentration [2]. Among all existing TFM geometries, the Clawpole TFM (CTFM) may be the one offering the best compromise between torque density and ease of construction and manufacturing [3]-[5]. CTFM magnetic circuits are usually made from soft magnetic composite materials (SMC) for their isotropic properties and for manufacturing purposes. A CTFM version using a hybrid stator made of a combination of SMC and Fe-Si laminations or amorphous material is presented in [4][6]. Compared to CTFMs made of SMC only, this configuration offers reduced iron losses while further improving its manufacturing. An exploded view of one phase of a 20 pole pair CTFM with hybrid stator is shown in Fig. 1.

High power and torque densities of TFMs are usually obtained with a large number of poles and high electric loadings. However, this also implies that optimized TFM designs are penalized by an inherent poor magnetic coupling (high leakage fluxes) which traduces in low power factors [2][3][5]. The key to adequate TFM designs is to minimize such unwanted leakage fluxes without reducing the mutual coupling between stator and rotor fluxes and the pole number. Therefore, leakage paths are crucial and cannot be neglected when designing a TFM. Unfortunately, 3D flux line patterns in the machine magnetic circuit, complex leakage paths and saturation significantly add to the complexity of TFM design.

Many reports of CTFM design methods can be found in the literature as in [2], [3], [5], [7], [8], [10]. As for any electrical machine design, the CTFM design process mainly consists in finding an optimal set of machine parameters while specific constraints are taken into account.

Due to the complex topology of CTFMs, finite element (FE) simulations are commonly used in the design process [2], [3], [10]. The 3D structure of the CTFM requires time consuming finite element analyses (FEA) that are not well suited to iterative optimization procedures. Therefore, CTFM design processes based on FEA often rely on simple cut and try experimentations guided by the designer's knowledge [3], [10]. It is the author's experience that such a design approach is time-consuming but also frustrating as there is no guarantee of convergence to one true optimal solution.

Analytical models are much better suited to such design and optimization processes as they are faster to solve and enable better exploration of the solution space. In [2], [10], simplified magnetic reluctance networks are used to derive CTFM flux and calculate the machine torque. As the models neglect leakage paths and saturation, significant errors are obtained restraining their use to the sole estimation of an initial value for subsequent FEA-based optimization process. Flux and torque values can also be evaluated with rather complex magnetic reluctance networks as those presented in [5], [7], [8]. Such reluctance networks model 3-D flux paths in the CTFM magnetic circuit and leakage paths as well through several reluctances. Flux paths and reluctance expressions are derived from several FEA [8], [9]. Despite their complexity, such models can be programmed to be employed in an optimization procedure as in [5]. The accuracy of such complex reluctance models is dependent on the machine dimensions: assumptions taken to model main and leakage paths are strongly related to the magnetic circuit shape and dimensions. While accurate for some machine designs, it can lead to significant errors for others. With complex reluctance models for flux estimation with 10

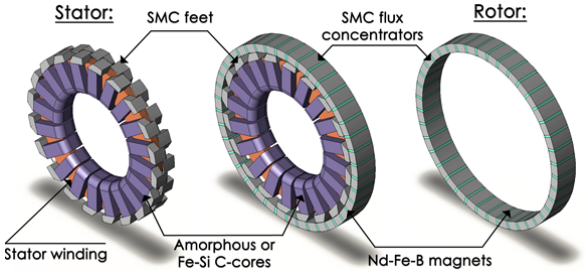

Fig. 1. 1 phase, 20 pole pairs CTFM with hybrid stator. Left: stator. Center: whole motor phase. Right: rotor.

different TFM designs, errors between analytical and FE results varying between -3 % and 25 % have been reported [9]. Hence, using such models in an optimization process can lead to false-optimal designs.

This presentation addresses the difficulty of modeling and optimizing TFMs by presenting the basis of a design method applied to the CTFM with hybrid stator structure. The method uses a magnetic model based on a reluctance network equipped with an error compensation mechanism. The correction factors are derived with 3D Finite Element Analysis and applied to some selected reluctances. The emphasis is put on the accuracy of the corrected reluctance network after compensation and its usefulness when applied in the machine optimization process.

The objective of the optimization procedure described in this communication is to maximize the no-load flux captured by the stator winding. For a given number of poles, maximizing the no-load flux will maximize the electromotive force and maximize the machine torque.

2. Clawpole Transverse-Flux Machine with Hybrid Stator

The characteristics and performances of a CTFM using a hybrid stator have been described in [4], [6]. The term “hybrid” refers to the use of two different magnetic materials in the stator. SMC are used in the regions contiguous to the airgap where a material with isotropic properties is required. Fe-Si laminations or amorphous C-cores are used around the stator winding. The hybrid stator configuration enables reducing the CTFM iron losses while simplifying its construction and manufacturing. The basic structure of one phase, 20 pole pairs CTFM with hybrid stator is shown in Fig. 1. It consists in:

- An external rotor with SMC flux concentrators and Nd-Fe-B magnets,
- An internal “hybrid” stator made of two parts with different magnetic materials: SMC stator feet and laminated or amorphous stator C-shaped cores.
- A ring-shaped phase coil.

As in previous works presented in [5], [7], [8], several FEA have been performed to identify flux paths across the machine magnetic circuit. The observation of flux vector distributions led us to the identification of the machine main flux path as well as its major leakage fluxes under load and no-load conditions.

A. CTFM main flux path

Fig. 2 shows the main flux path across one CTFM pole pair without considering leakage fluxes. Main flux path across the magnetic circuit can be described as mainly flowing:

- Circumferentially through the rotor magnets.
- In a 3-D way through the rotor concentrators.
- Radially in the airgap.

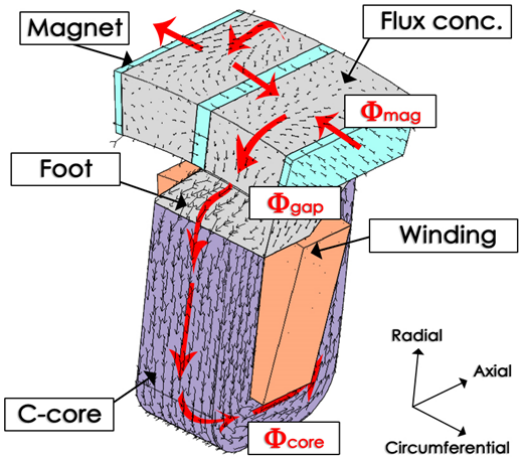

Fig. 2. CTFM main flux path across one pole pair, excluding leakage fluxes at no-load condition.

- In a 3-D space through the stator feet.
- In an axial-radial plane through the stator core.

As depicted in Fig. 2, let us consider Φ_{mag} as the flux crossing the magnet surface, Φ_{gap} as the flux across the airgap and Φ_{core} as the one passing through the stator core section, being also the machine no-load flux.

B. CTFM leakage fluxes

As mentioned earlier, a non-negligible part of the flux produced by the rotor magnets or the stator winding do not travel through the whole magnetic circuit. The latter can be qualified as leakage fluxes. Their prediction is crucial for the design of CTFMs. 4 major leakage paths have been identified by observation of FEA simulations:

- Rotor PM leakage Φ_{leakR}

A part of the flux produced by the magnets does not go through the concentrators. Instead, it leaks in non-magnetic regions around the magnets as shown in Fig 3. Rotor PM leakage flux Φ_{leakR} mainly occurs in axial-radial planes above the rotor and in the airgap. It also leaks in axial-circumferential planes from both sides of a rotor phase.

- Stator-rotor leakages $\Phi_{leaksided}$ and $\Phi_{leaksidep}$

Some of the magnet flux crossing the airgap does not link the stator winding and leaks from both axial sides of the stator feet as shown in Fig 3. One part of this leakage flux, $\Phi_{leaksided}$, leaves/returns to the magnet from the right part of a foot facing a concentrator (straight side of a foot). The other part, $\Phi_{leaksidep}$, leaves/returns to the magnet from the left part of a foot (skewed side of a foot).

- Stator leakage between adjacent feet Φ_{leakS}

A part of the magnet and armature flux does not contribute to the torque production as it takes a return path in the region between two adjacent feet as shown in Fig. 4. At no-load, this leakage flux is very small and can almost be neglected.

From the identification of the main and leakage flux paths, a magnetic model for the determination of the machine no-load flux Φ_{core} has been built.

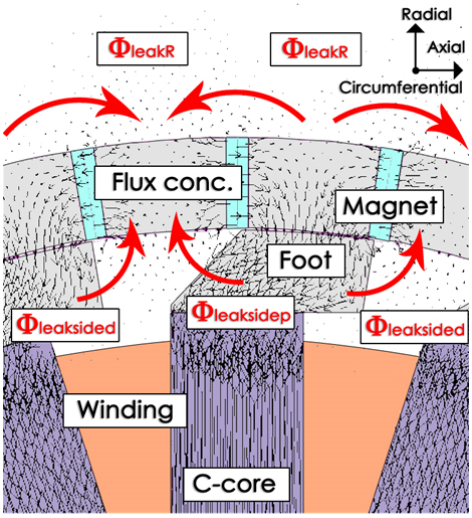

Fig. 3. Stator-rotor leakages $\phi_{leaksided}$ and $\phi_{leaksidep}$ through the airgap between a foot and adjacent concentrators.

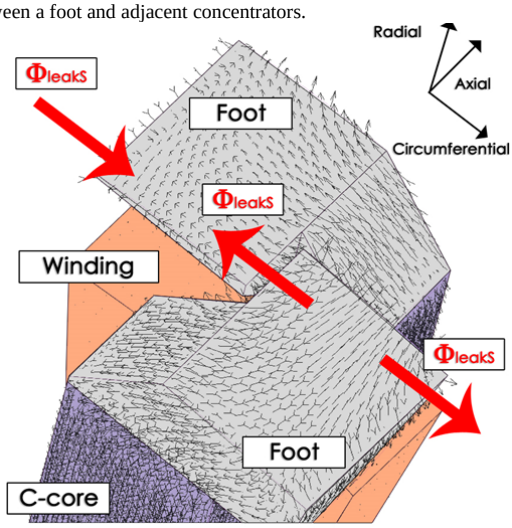

Fig. 4. Leakage occurring between 2 stator feet.

3. Magnetic Model used for the determination of the no-load flux linkage

The method described in this paper uses a magnetic reluctance network in order to evaluate the no-load flux linking the machine winding. Considering the motor symmetry, this model can be reduced to one pole pair only. Fig. 5 shows the proposed reluctance model derived.

A Microsoft Excel worksheet has been used at this point, where all the machine geometrical parameters can be entered as inputs to the computation process. The

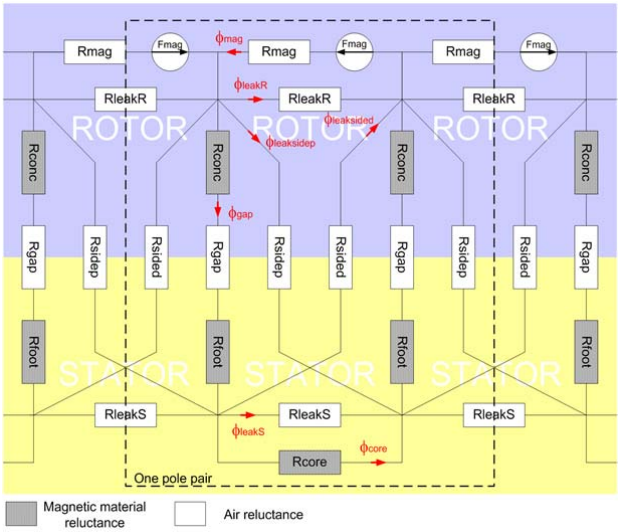

Fig. 5. Equivalent magnetic reluctance network used for the determination of the CTFM no-load flux-linkage.

expressions of the reluctances described in this section have also been implemented in the Microsoft Excel® worksheet.

4. Model error Compensation is a Design Process

Within the Excel-Based optimization loop, where the geometrical parameters are varied, correction factors are implemented and applied to the CTFM electrical parameters computed from the reluctance network. These factors are adjusted from the differences observed between the analytical model outputs and those calculated from 3D Finite Element Analysis.

This design process has been implemented in a Microsoft Excel® worksheet for a better usability and automation purpose. Flux calculations with the reluctance network, considering non-linear material characteristics, are achieved using algorithms developed

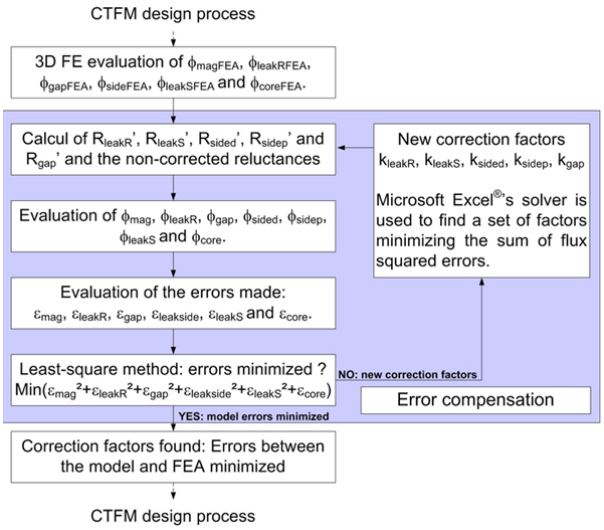

Fig. 6. Flowchart describing the least-square minimization method used by the error compensation mechanism to determine the correction factors.

in Visual Basic macros. The compensation error mechanism has been implemented in the worksheet to work in pair with the magnetic model. Visual Basic macros have also been developed to link worksheet data to the FE software Infolytica® Magnet VI® in order to build, simulate and get results from FE models. Using Microsoft Excel®'s solver, the developed worksheet acts as a simple and powerful CTFM design tool. Fig. 7 shows the interactions between Microsoft Excel®, the Visual Basic macros and Infolytica® Magnet VI® in the developed tool.

As previously indicated, the objective of the optimization process is to maximize the no-load flux per pole Φ_{Core}. The graph presented in Fig. 8 shows the variation of the optimized Φ_{Core} calculated with the analytical model over the whole design process. It also presents the corresponding no-load flux obtained from FEA used for validation in the error compensation process.

5. Design method computation time

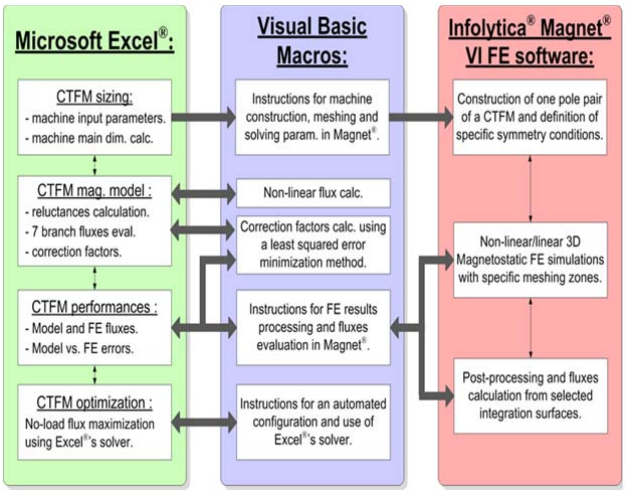

Fig. 7. Hierarchic diagram describing the interactions between Microsoft Excel®, the Visual Basic macros and Infolytica® Magnet VI® used for the development of the CTFM design method.

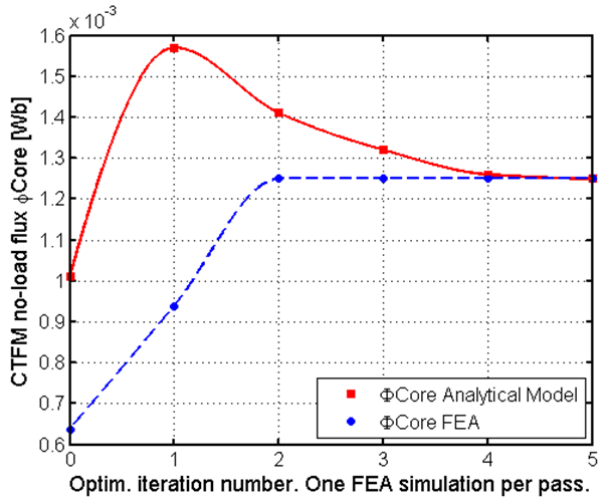

Fig. 8. Variation of the saturated no-load fluxes estimated analytically and with FEA during the whole design process.

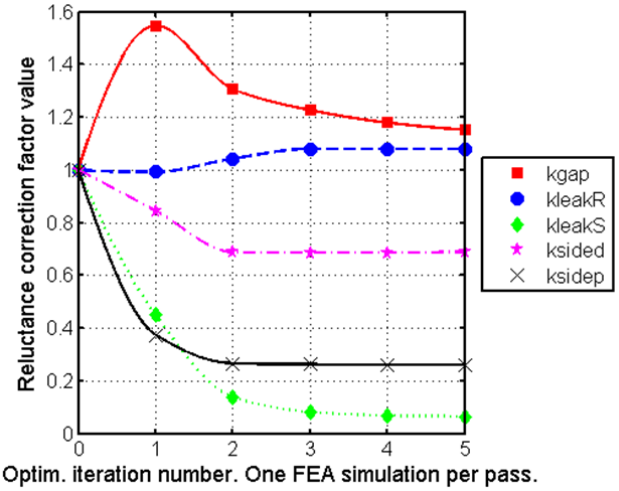

Fig. 9. Variation of the correction factors k_{gap}, k_{leakR}, k_{leakS}, k_{sided} and k_{sidep} during the design process.

With the example considered here, 5 optimization iterations were required for a total of 5 FE simulations in 3-D. With this method, 4 to 6 iterations are generally sufficient for a whole CTFM design process. Obviously, the time required for the maximization of a CTFM no-load flux mostly depends on the number of FE simulations required, the FE mesh settings but also the size of the CTFM.

For FE simulations, a particular attention is paid to refine the mesh in airgap and leakage regions for sufficient accuracy. In the example presented here, a mesh containing more than 730 000 elements has been considered. Run on a 2.61 GHz Athlon® processor, each FE simulation requires almost 15 minutes. The analytical determination of the saturated no-load flux as well as the use of Excel®'s solver do not require more than 1 minute per pass. Therefore, the design process total duration for the example considered here is about 80 minutes, providing an accurate solution within acceptable simulation time.

6. Optimality of the solutions obtained with the method described

The question of the optimality of the solutions obtained with the method described in this paper should be addressed. In other words, it must be verified if the optimization method and the analytical model are efficient enough to avoid convergence to local optimum in the solution space. As there is no evident mathematical way to prove this, a more practical approach has been followed.

8 different CTFM optimization parameter sets (k_{smag}, k_{rot}, k_{ap}, k_{cp}, k_{rp}, k_{hb}, k_{hp} and k_{pn}) have been selected as initial parameters for 8 design processes. R_a = 1000 mm,

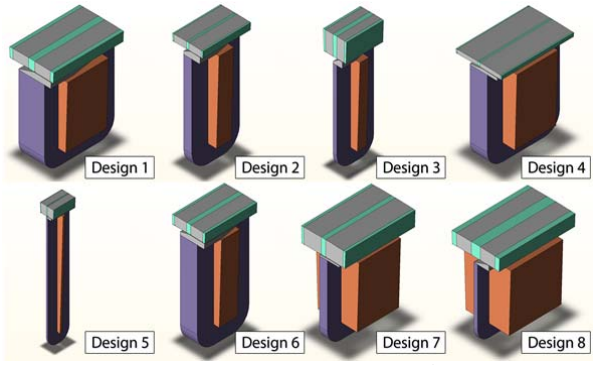

Fig. 10. 8 CTFM designs chosen as initial designs before optimization.

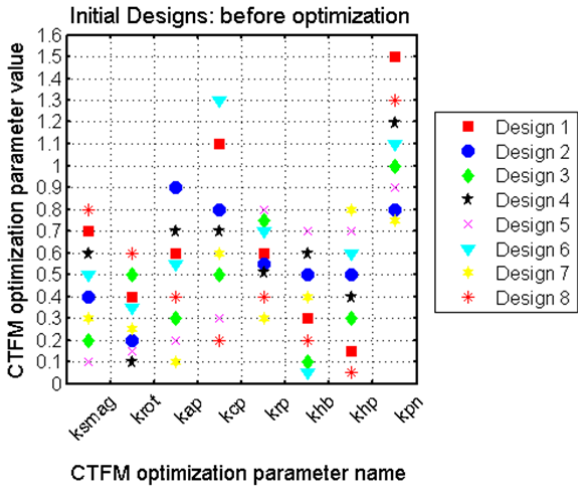

Fig. 11. CTFM parameters k_{smag}, k_{rot}, k_{ap}, k_{cp}, k_{rp}, k_{hb}, k_{hp} and k_{pn} chosen as initial values of 8 design processes.

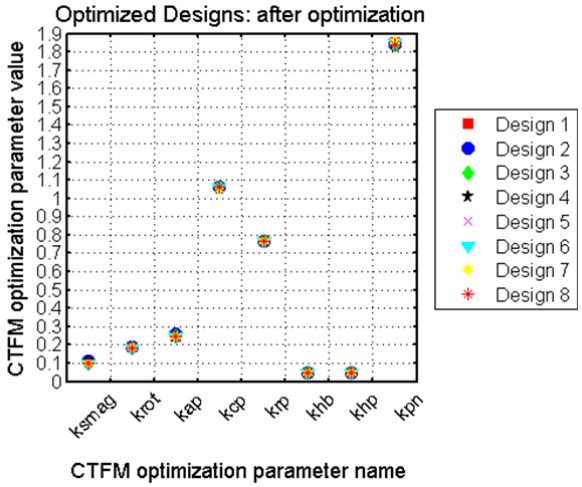

Fig. 12. CTFM optimal parameters k_{smag}, k_{rot}, k_{ap}, k_{cp}, k_{rp}, k_{hb}, k_{hp} and k_{pn} of 8 designs found after no-load flux maximization before error compensation.

airgap = 0.8 mm, axial length = 100 mm, p = 100 and $A_{winding}$ = 5000 mm². Fig. 10 presents illustrations of these 8 initial designs. Fig. 11 shows a graph representing their corresponding 8 initial optimization parameters sets (Design 1 to Design 8).

The corresponding 8 optimal sets of parameters after the no-load flux maximization are shown in Fig. 12 (Design 1 to Design 8). One can notice that the 8 optimization problems nearly converged to the same solution: the same parameter set (k_{smag} = 0.11, k_{rot}= 0.19, k_{ap}= 0.25, k_{cp}= 1.06, k_{rp}= 0.77, k_{hb}= 0.05, k_{hp}= 0.05 and k_{pn}= 1.84) has been found as the optimal set maximizing the no-load flux starting from 8 different initial parameter sets. Only small biases are observed between the designs: for example, the optimal value of k_{smag} has been found equal to 0.11 for Design 1 while it converged to 0.10 for Design 8. As the same optimal parameter set has been found since the first design step for the 8 designs, it is expected that similar correction factors will be obtained during the design process. Similarly, same final optimal parameters are expected at the end of the design process in the 8 cases. It is therefore not necessary to continue the design process until FEA iteration #5.

As this observation does not constitute a proper mathematical proof, it still provides us good confidence on the optimality of the solutions found with the design method.

7. References

[1] Weh H., May H., "Achievable Force Densities for PM Excited Machines in New Configurations", in *Int. Conf. on Elec. Mach. - ICEM, pp. 1107-1111, Sept. 1986, München, Germany.*

[2] Viorel I.-A., Henneberger G., Blissenbach R., Löwenstein L., "Transverse Flux Machines. Their Behaviour, Design, Control and Applications", *Mediamira 2003, Cluj, Romania.*

[3] Maddison C.P., Mecrow B.C. and Jack A.G, "Claw Pole Geometries For High Performance Transverse Flux Machines", *Int. Conf. on Elec. Mach. ICEM, pp. 340-345, Sept. 98, Vigo, Spain.*

[4] Dubois M.R., Dehlinger N., Polinder H., Massicotte D., "Clawpole Transverse Flux Machine with Hybrid Stator", in *Int. Conf. on Elec. Mach. - ICEM, paper 412, Sept. 2006, Chania, Greece.*

[5] Dickinson P.G., Jack A.G., Mecrow B.C., "Improved Permanent Magnet Machines with Claw Pole Armatures", in *Int. Conf. on Elec. Mach. - ICEM, pp. 1-5,Aug. 2002, Bruges, Belgium.*

[6] Dehlinger N., Dubois M.R., "Clawpole Transverse Flux Machine with Amorphous Stator Cores", in *Int. Conf. on Elec. Mach. - ICEM, paper 1017, Sept. 2008, Vilamoura, Portugal.*

[7] Ibala A., Masmoudi A., Atkinson G., Jack A.G. , "A New Reluctance Model of a Claw Pole TFPM using SMC for the Magnetic Circuit", in *Int. Conf. on Eco. Vehic. and Ren. Ener. - EVER, March 2009, Monte Carlo, Monaco.*

[8] Ibala A., Masmoudi A., Atkinson G., Jack A.G. , "Investigation of the Leakage Fluxes of SMC Made Magnetic Circuit Claw Pole TFPM", in *Int. Conf. on Eco. Vehic. and Ren. Ener. -EVER, March 2009, Monte Carlo, Monaco.*

[9] Dubois M.R.., "Optimized Permanent Magnet Generator Topologies for Direct-Drive Wind Turbines", *PhD Thesis, Delft University of Technology, Delft, The Netherland, 2004.*

[10] Blissenbach R., "Entwicklung von Permanenterregten Transversalflussmaschinen hoher Drehmomentdiche für Traktionsantriebe", *PhD Thesis, RWTH Aachen, Oct. 2002, Aachen, Germany* [In German].